The Canadian Mineralogist
Vol. 37, pp. 127-142 (1999)

ZONING AND SUBSTITUTIONS IN Co–Ni–(Fe)–PGE SULFARSENIDES FROM THE MOUNT GENERAL'SKAYA LAYERED INTRUSION, ARCTIC RUSSIA

ANDREI Y. BARKOV[1]

Department of Earth and Planetary Sciences, McGill University, 3450 University Street, Montreal, Quebec H3A 2A7

YVES THIBAULT[1]

Department of Earth Sciences, University of Western Ontario, London, Ontario N6A 5B7

KAUKO V.O. LAAJOKI

Department of Geology, Institute of Geosciences, University of Oulu, FIN-90570 Oulu, Finland

VICTOR A. MELEZHIK AND LARS P. NILSSON

Geological Survey of Norway, P.O. Box 3006, Leiv Erikssons vei 39, N-7002 Trondheim, Norway

Abstract

Compositions, zoning patterns and element correlations in platinum-group element (*PGE*)–Co–Ni–Fe sulfarsenides from the Mount General'skaya complex, in Arctic Russia, reveal the following. (1) Members of the cobaltite–gersdorffite series (*MCGS*) form an extensive solid-solution series between relatively S-rich CoAsS and $(Ni_{0.667}Fe_{0.333})AsS$, and Ni–Fe order probably exists in their crystal structure. Co increases, whereas Ni–(Fe), *PGE*, X_{Rh} [100Rh/(Rh + Pd)] and the ratio As/S (atom.%) decrease toward the edge in the cryptically zoned *MCGS*. (2) The *PGE* are relatively enriched in the earlier sulfarsenide phases (typically in the core). (3) Ir–(Pt) is more effectively partitioned into the earliest phase than Rh; Rh is more strongly partitioned into the core than Pd, and transition metals are concentrated in the latest (marginal) phases. (4) The *PGE* substitute for Co, not for Ni and Fe in the *MCGS*. (5) Similar to Ni and Fe, the *PGE* correlate positively with As (and the As/S) and negatively with S, and they are selectively incorporated in relatively As-rich (S-poor) *MCGS*. In contrast, Co displays a strong negative correlation with As, and a positive one with S. A link seems to exist between cation and (di)-anion substitutions in the *MCGS*, and the incorporation of the *PGE* and other metals probably is controlled by charge balance. The higher temperature of crystallization of Ir–(Pt)AsS *versus* RhAsS, of RhAsS *versus* (Rh,Pd)AsS, and of (*PGE*)AsS *versus MCGS* may be crucial to form the zoning patterns and compositional trends of these sulfarsenides.

Keywords: platinum-group elements, platinum-group minerals, cobaltite–gersdorffite, sulfarsenides, isomorphous substitutions, zoning, mafic–ultramafic rocks, layered intrusion, Mount General'skaya, Kola Peninsula, Russia, Fennoscandian Shield.

Sommaire

Nous avons étudié les compositions, les schémas de zonation et les corrélations parmi les éléments dans les sulfarséniures à éléments du groupe du platine (*EGP*) – Co – Ni – Fe provenant du complexe du mont General'skaya, dans l'Arctique russe. Il en découle que (1) les membres de la série cobaltite–gersdorffite (*MSCG*) forment une solution solide étendue entre CoAsS relativement enrichi en soufre et $(Ni_{0.667}Fe_{0.333})AsS$; une mise en ordre impliquant Ni et Fe existerait dans la structure cristalline. La teneur en Co augmente, tandis que Ni–(Fe), les *EGP*, X_{Rh} [100Rh/(Rh + Pd)] et le rapport As/S (% atomique) diminuent vers la bordure des cristaux de *MSCG* zonés de façon cryptique. (2) Les *EGP* sont relativement enrichis dans les sulfarséniures précoces, typiquement disposés près du coeur des grains. (3) Ir–(Pt) est plus effectivement réparti dans la fraction précoce que le Rh; à son tour, le Rh est plus fortement concentré dans le coeur que le Pd, et les métaux de transition sont plutôt concentrés dans les phases tardives, à la bordure des grains. (4) Les *EGP* prennent la place du Co, et non du Ni et du Fe dans le *MSCG*. (5) Tout comme le Ni et le Fe, les *EGP* montrent une corrélation positive avec l'arsenic, et avec le rapport As/S, et une corrélation négative avec le soufre, et ils seraient préférentiellement incorporés dans la fraction de *MSCG* relativement riche en arsenic (et pauvre en S). En revanche, le Co fait preuve de fortes corrélations négative avec l'arsenic et positive avec le soufre. Un lien semble exister entre les substitutions impliquant les cations et les (bi)-anions dans le *MSCG*, de sorte que l'incorporation des *EGP* et autres

[1] *E-mail addresses*: barkov@geosci.lan.mcgill.ca, ythibaul@julian.uwo.ca

cations serait régie par l'équilibre électrostatique. Les températures élevées de cristallisation de Ir–(Pt)AsS *versus* RhAsS, de RhAsS *versus* (Rh,Pd)AsS, et de (*PGE*)AsS *versus MSCG* pourraient s'avérer très importantes pour expliquer les schémas de zonation et les vecteurs de composition de ces sulfarséniures.

(Traduit par la Rédaction)

Mots-clés: éléments du groupe du platine, minéraux du groupe du platine, cobaltite–gersdorffite, sulfarséniures, substitutions isomorphes, zonation, roches mafiques–ultramafiques, complexe stratiforme, mont General'skaya, péninsule de Kola, Russie, bouclier fennoscandien.

Introduction

Sulfarsenides of transition metals, cobaltite (ideally CoAsS) and gersdorffite (NiAsS), form extensive solid-solutions that involve arsenopyrite (FeAsS), both in experimental (Klemm 1965) and natural (*e.g.*, Béziat *et al.* 1996) systems. Platinum-group-element *PGE* sulfarsenides, hollingworthite (ideally RhAsS; Stumpfl & Clark 1965), irarsite (IrAsS; Genkin *et al.* 1966), and platarsite (PtAsS; Cabri *et al.* 1977) belong to the cobaltite group of minerals. Extensive solid-solutions in the hollingworthite – irarsite – platarsite system have been documented. There is also considerable solid-solution between the sulfarsenides of the *PGE* and Co–Ni–(Fe), which is favored by their structural similarities. However, members of the cobaltite–gersdorffite series (*MCGS*) containing essential *PGE* are very rare in nature (Cabri & Laflamme 1976, Distler & Laputina 1979, Barkov *et al.* 1996, Gervilla *et al.* 1997). Isomorphous substitutions in *PGE*-bearing *MCGS* have not previously been characterized through element correlations.

In this paper, we report occurrences of Co–Ni–(Fe)–*PGE* sulfarsenides from the Mount General'skaya layered intrusion, with emphasis on their patterns of zoning, which have important implications for partitioning of the *PGE* in natural sulfarsenide systems and for substitutions in the sulfarsenides.

The Proterozoic Mount General'skaya (or Luostari) mafic intrusion in the Kola Peninsula, Russia, seems to be the northernmost layered intrusion in the Fennoscandian Shield (Fig. 1). A Sm–Nd age of 2453 ± 42 Ma, ε_{Nd} (T) = –2.3 ± 0.4 (Bakushkin *et al.* 1990) and a Pb–Pb zircon age of 2505.1 ± 1.6 Ma (Amelin *et al.* 1995) for the Mount General'skaya complex are internally consistent. The intrusion is a wedge-shaped, northeast-trending body ~4 km long and up to ~1 km in maximum thickness. Its width decreases in the northeast direction from ~3 to ~0.5 km. The intrusion cuts

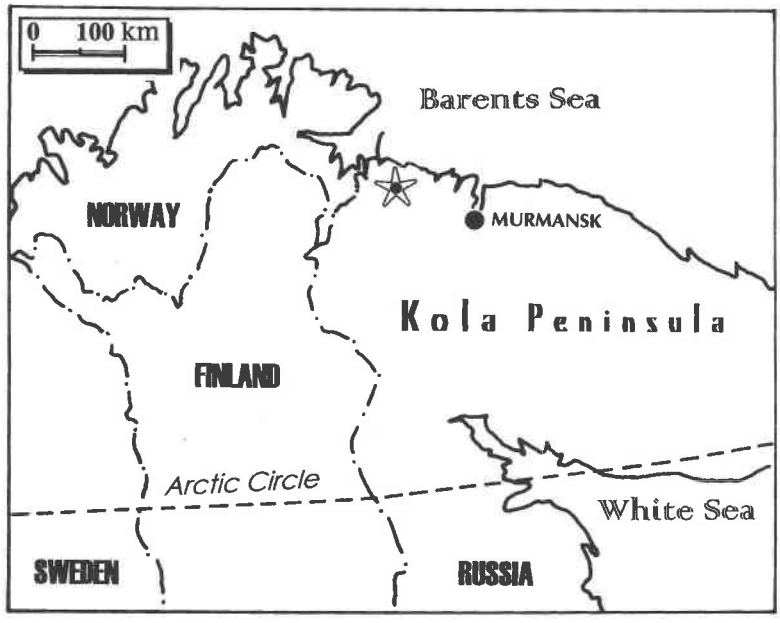

FIG. 1. Location of the Mount General'skaya layered intrusion (shown by star) in Arctic Russia.

Archean granite gneisses and is overlain by basal polymictic conglomerates of the Early Proterozoic Pechenga Supergroup of sedimentary and volcanic rocks. The Mount General'skaya complex is predominantly composed of various gabbronorites and gabbro, which are widely altered to various degrees. Some olivine-bearing cumulates are present at a lower stratigraphic level. Base-metal sulfide (*BMS*) mineralization occurs within several layers in the intrusion (Yakovlev 1971, Bakushkin 1979). Palladium is the principal *PGE*, and the ratio Pd:Pt in the mineralized zones is typically greater than 5. The presence of *PGE* in solid solution in *MCGS* in the intrusion was first noted by Barkov *et al.* (1990). Barkov *et al.* (1994) described various platinum-group minerals (*PGM*) from the Mount General'skaya complex.

Occurrence

The Co–Ni–(Fe)–*PGE* sulfarsenides are associated with disseminated *BMS* (up to 15–20 modal %) in variously altered gabbroic rocks. The *BMS* assemblage consists of varying amounts of chalcopyrite, pyrrhotite, pentlandite (main *BMS*) and pyrite. Less common and relatively rare ore minerals are the *MCGS*, argentopentlandite, hessite, altaite, sphalerite, Se-rich members of the galena–clausthalite series, Au–Ag alloy ($Au_{65-69}Ag_{31-35}$), molybdenite, pilsenite (?) and a Bi–Te–Se–S phase. Most of these minerals typically occur in spatial association with *PGM*. A member or members of the linnaeite group and Ni-rich mackinawite are common secondary base-metal sulfides. Apatite is a common accessory mineral in the *BMS*-bearing rocks.

The *PGM* (<5 μm to ~0.1 mm) mainly occur at the boundaries between the *BMS* and hydrous silicates, and as inclusions in the latter. However, grains hosted by the *BMS* also are widespread. The *PGM* are predominantly members of the merenskyite $Pd(Te,Bi)_2$ – palladian melonite $(Ni,Pd)(Te,Bi)_2$ series, (Sb-rich) kotulskite Pd(Te,Bi) and sperrylite $PtAs_2$, plus minor michenerite PdTeBi, hollingworthite, and a very rare Pd-rich bismuthotelluride, probably Bi-rich telluropalladinite $[Pd_{9.08}(Te_{2.99}Bi_{0.93})_{\Sigma 3.92}]$.

The *MCGS* are quite abundant accessory minerals in the *BMS*-bearing rocks. They commonly occur as inclusions within various *BMS* (predominantly in chalcopyrite, more rarely in pyrrhotite and pentlandite), at the contact between the *BMS* with hydrous silicates, and rarely isolated within secondary silicates. Their intergrowths with merenskyite–melonite are common. The grain size of the *MCGS* varies from ≤5 μm to 0.1 mm, but some crystals, associated with late-stage (veinlet-like) *BMS*, were found to reach 0.2 to 0.3 mm. The *MCGS* are typically subhedral to euhedral; anhedral grains also are present, however. A zoned sulfarsenide grain occurs in a *BMS*-rich altered rock, in a strongly unusual spatial association with abundant zircon, and with a rare-earth-element-rich mineral, allanite-(Ce). These contrasting mineral assemblages imply a local enrichment in both the *PGE* and incompatible lithophile elements in the environment. However, other zoned sulfarsenides are not necessarily associated with this or similar mineral assemblages.

Textural Characteristics

Patterns of zoning

More than ten zoned sulfarsenide crystals, inclusions in various *BMS* (*e.g.*, Figs. 2, 3), were characterized by scanning-electron microscopy (SEM) and electron-microprobe analysis, using wavelength-dispersion (WDS) and quantitative energy-dispersion (EDS) spectrometry.

Two main types of zoning (I and II) were defined. Grains displaying characteristics of both of these types (intermediate zoning) also were observed. A cryptic compositional zoning with respect to *PGE*, Co, Ni and the ratio As/S (type I) is invisible under microscope. The zones may differ strongly in composition, and are readily recognized by back-scattered electron imaging and X-ray mapping for base metals and the *PGE* (Figs. 2 to 4). The zones most enriched in *PGE* typically, but not necessarily, occur in the central parts of the grains and show rather diffuse boundaries with the surrounding *MCGS* (Figs. 2a, b), which may also contain essential *PGE* in solid solution. An example of well-developed growth zoning is shown in Figure 2a. The zones are subparallel to crystal faces, and show a general decrease in mean atomic number toward the edge.

Type-II zoning is represented by composite grains, consisting of Ni–Co-poor (or Ni–Co-free) hollingworthite–irarsite (core) and *PGE*-poor *MCGS* (periphery). The latter is not zoned with respect to the *PGE*. Unlike the grains with type-I zoning, rather sharp phase-boundaries, visible under the microscope in larger grains, are characteristic of the type-II zoning. A homoaxial, type-II zoned grain in Figures 2d and 2e comprises an internal crystal with the highest mean atomic number (Hol-1), which is hosted by a crystal with a lower mean atomic number (Hol-2), and the latter is surrounded by a *MCGS*. The internal phases exhibit well-developed outlines.

An example of the intermediate zoning is shown in Figure 2c. The grain consists of subhedral (Ni–Co-poor) osmian hollingworthite, which is surrounded by a cryptically zoned grain of *MCGS*. The latter displays remarkable (*PGE*-enriched) growth-zones (diffuse and lighter in the back-scattered-electron image). In addition, grains of *MCGS* containing hollingworthite inclusions (commonly, but not necessarily, in the core) also were observed.

Complementary textural relationships

The *MCGS* often occur as intimate intergrowths with Pd–Ni bismuthotellurides (merenskyite–melonite

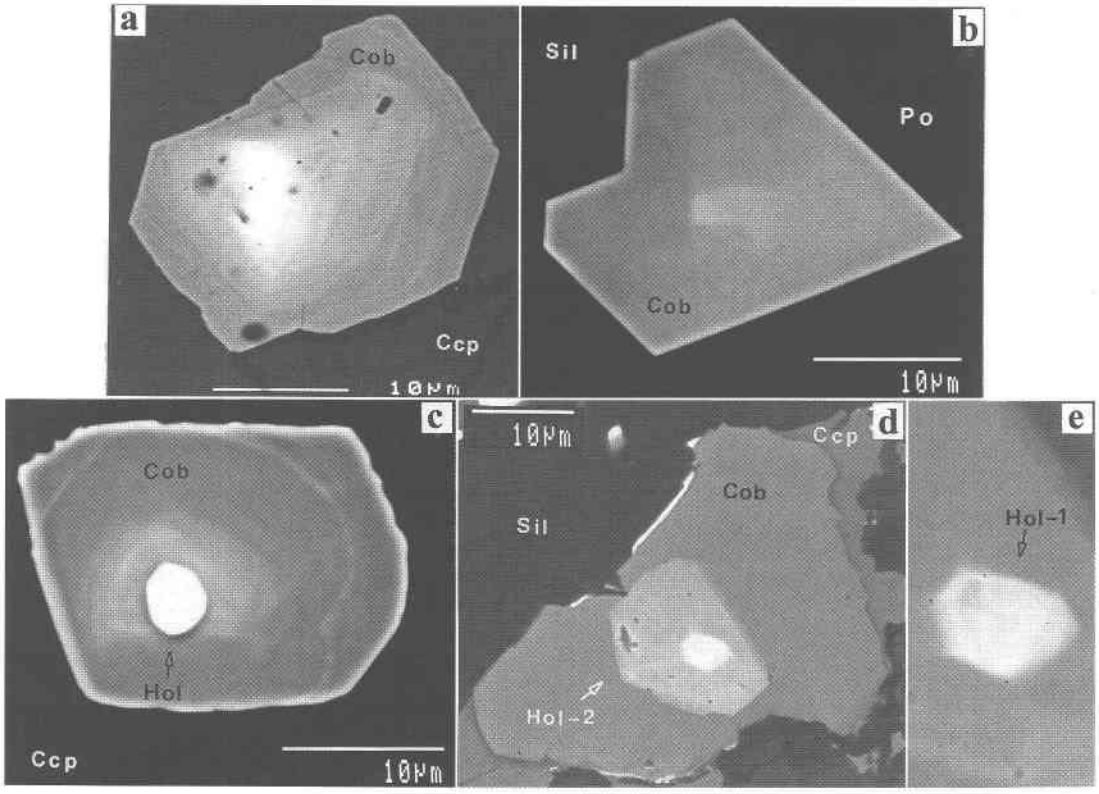

FIG. 2. (a) Cryptically zoned cobaltite–gersdorffite–(hollingworthite) crystal (Cob). Note the *PGE*-rich zone (white). (b) Euhedral cobaltite–gersdorffite (Cob), containing a diffuse, *PGE*-bearing zone in the center (light). (c) *PGE*-rich cobaltite–gersdorffite (Cob), showing growth zones around a subhedral grain of Os-rich hollingworthite (Hol). (d) Complexly zoned grain containing (from center to edge): euhedral Ir-rich hollingworthite (Hol-1), Ir-free hollingworthite (Hol-2), and *PGE*-poor cobaltite–gersdorffite (Cob). (e) Magnification of area in Figure 2d showing the central crystal (Hol-1). Ccp: chalcopyrite, Po: pyrrhotite, and Sil: hydrous silicate. Back-scattered electron (BSE) images.

series), implying that these minerals belong to the same paragenetic association, and display complementary replacement-induced relationships with these bismuthotellurides (Fig. 5). However, an essential *PGE*-enrichment does not necessarily occur in those *MCGS* that are intergrown with the *PGM*. Textural data imply a relatively late timing for the formation of the *MCGS*–merenskyite intergrowths in the crystallization history (Fig. 5).

ANALYTICAL METHODS

The WDS analyses of the sulfarsenides were carried out with a JEOL JXA–8600 electron microprobe, operated at an accelerating voltage of 25 kV and a probe current of 30 nA. Counting periods were 20 to 40 s. X-ray lines (and standards) used were Ni$K\alpha$ (synthetic NiS), Fe$K\alpha$ (FeS), Co$K\alpha$, Rh$L\alpha$, Pd$L\beta$, Ir$L\alpha$, Pt$L\alpha$, Os$M\alpha$, Ru$L\alpha$ (pure metals), As$L\alpha$, and S$K\alpha$ (FeAsS). The Pd$L\beta$ line was used instead of Pd$L\alpha$ in order to eliminate overlap between emission lines of Rh and Pd. We also used the As$L\alpha$ line, not the $K\alpha$ line, because the latter overlaps with lines of some of heavy *PGE*. Major problems due to overlap were not experienced during this study; nevertheless, all possible overlaps were checked by a careful analysis of the standards and corrected, including the Rh$L\alpha$–Ru$L\beta$ overlap. The minimum detection-levels are ≤0.02 for Fe, Co, and Ni, 0.03 for Ru, 0.04 for Rh, 0.05 for Os, 0.06 for As, 0.07 for Ir, 0.08 for Pd, and 0.09 wt.% for Pt. Merenskyite also was analyzed with the JEOL–8600 microprobe, operated at 20 kV and 25 nA (25 kV and 35 nA for Pt and Rh); the $K\alpha$ line was used for Ni and Fe, the $L\beta$ line for Pd, and the $L\alpha$ line for Pt, Te and Bi. Pure elements were used as standards.

For comparison, WDS analyses of one of the cryptically zoned crystals (Fig. 2a) were obtained with a Cameca Camebax electron microprobe, operated at an

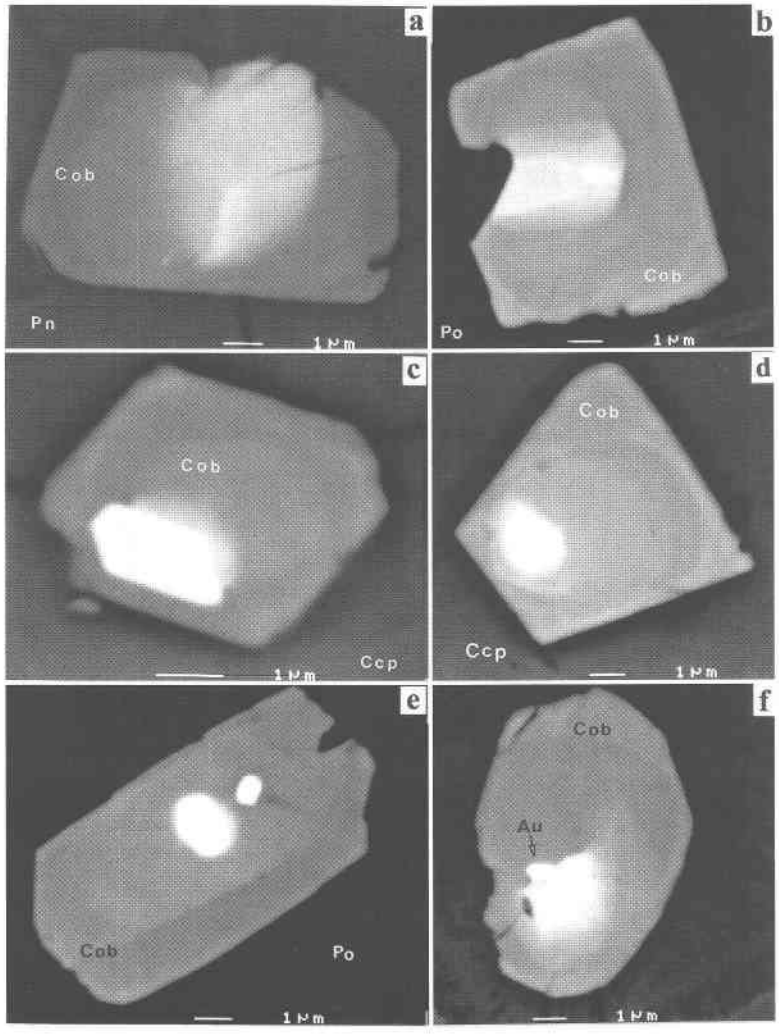

FIG. 3. (a–f) Zoned cobaltite–gersdorffite–*PGE* sulfarsenide crystals (Cob), enclosed by pentlandite (Pn), pyrrhotite (Po) and chalcopyrite (Ccp). The *PGE*-rich zones are white. The crystal in Figure 3f is located within a secondary base-metal sulfide after pentlandite and contains a minute inclusion of a gold-rich telluride (?) (Au). Note a relative enrichment in heavy *PGE* in tiny zones (white) in the center (Figs. 3a, b, f). BSE images.

accelerating voltage of 20 kV and a probe current of 22 nA. X-ray lines (and standards) used were Ni*K*α, Fe*K*α (FeS_2), Co*K*α, Rh*L*α, Pd*L*α, Ir*L*α, Pt*M*β, Os*M*α (pure metals), As*L*α (synthetic GaAs), and S*K*α (FeS_2). The results were processed by a "PAP" on-line program and, because of lower totals, were normalized to 100 wt.%. An additional correction for interference between Pd*L* and Rh*L* emission lines was made.

The EDS analyses were carried out at 15 kV and 1.2 nA, using a JEOL JSM–6400 scanning electron microscope, equipped with a LINK eXL energy-dispersion spectrometer. The lines (and standards) used were Rh*L* (pure Rh and synthetic RhSb), Pt*M*, Os*M*, Ir*M*, Pd*L*, Co*K*, Ni*K*, Fe*K*, Bi*M* (pure elements), As*L* ($PtAs_2$), S*K* (pyrite) and Te*L* ($PtTe_2$). The most finely focused beam (~1 μm) was applied in both the EDS and WDS analyses. Counting periods were 100 s, and the spectra were processed by ZAF–4 and Link ISIS (version 3.2) on-line programs.

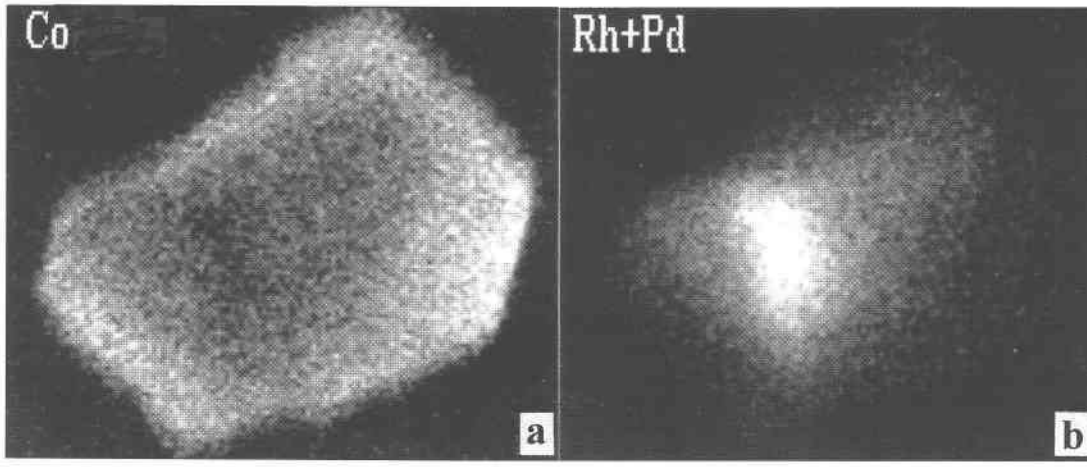

FIG. 4. Cobalt (a) and Rh + Pd (b) X-ray maps of a zoned crystal of Co–Ni–(Fe)–*PGE* sulfarsenides (see BSE image in Fig. 2a).

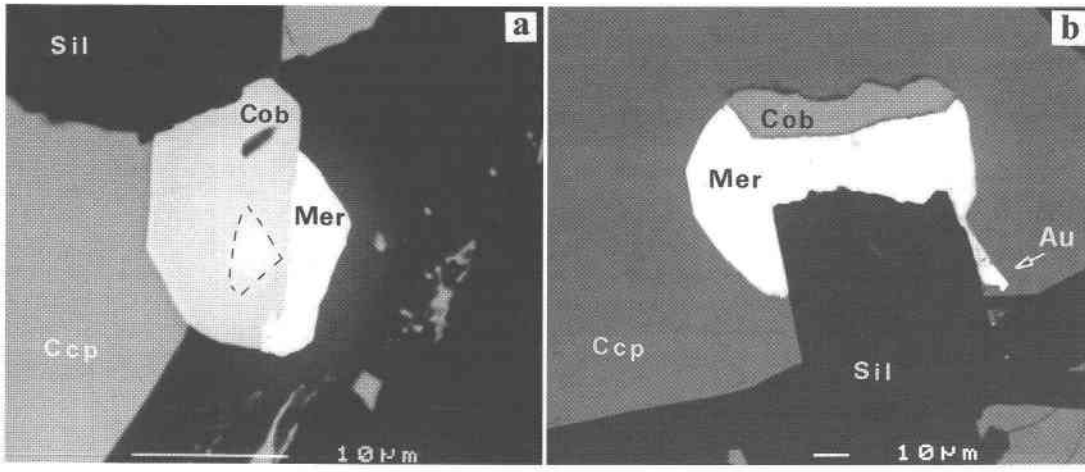

FIG. 5. BSE images showing complementary textural relationships between cobaltite–gersdorffite and merenskyite. (a) Cobaltite–gersdorffite, Cob, (*PGE*-rich zone is outlined in dashed line), surrounded by a partial rim of merenskyite (Mer). (b) Merenskyite (Mer) rimmed partially by cobaltite–gersdorffite (Cob). Symbols: Ccp: chalcopyrite, Sil: hydrous silicate, Au: Au–Ag alloy.

COMPOSITIONAL VARIATIONS

Electron-microprobe traverses

Three cryptically zoned crystals (type-I and intermediate zoning) were analyzed along point traverses (Fig. 6). Three sets of analytical data for one of these crystals (Fig. 6a) were obtained using various electron-microprobe facilities. They are presented in Tables 1 to 3 and in variation diagrams (Fig. 7), and are internally consistent. Very strong compositional variations are observed, but the diffuse core and immediately adjacent areas do not strongly contrast in composition. The core shows the highest content of all *PGE*, two of which (Rh and Pd) are dominant, and the low levels of Co and Ni, corresponding to a transitional member in the hollingworthite – cobaltite – gersdorffite series. The other zones are Rh–Pd-rich cobaltite or gersdorffite. The content of the *PGE* gradually decreases outward, and all of the *PGE* vary sympathetically with each other and with the ratio As/S, and together they vary antipathetically with Co (Fig. 7). In contrast, the concentration of Co progressively increases toward the edge, and the outermost zone shows an extreme enrichment in Co. Beyond

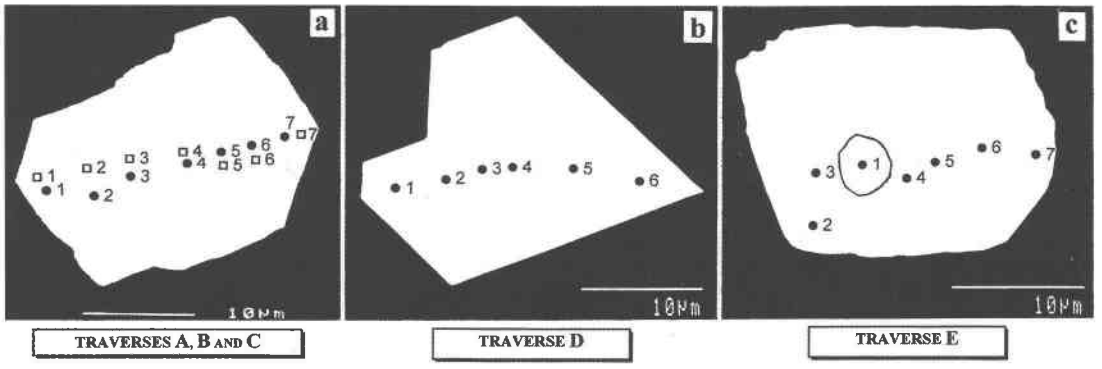

FIG. 6. Location of electron-microprobe traverses across cryptically zoned Co–Ni–(Fe)–*PGE* sulfarsenide crystals (BSE images are shown in Figs. 2a–c). Traverse A (solid circles): JEOL–8600 electron microprobe; traverse B (open squares): EDS analyses. Traverse C (Cameca Camebax electron microprobe) coincides with A and B and contains eight data-points (open diamonds; see Fig. 7).

the Ni–Fe-poor core, both Ni and Fe decrease toward the edge, as do the *PGE*. The low Fe in the point analyses near the margins indicates that there was no interference from the Fe–(S)-rich host during the analyses. All the analytical facilities applied reveal covariation of the ratios X_{Rh} [100Rh/(Rh + Pd)] and As/S, both of which reach their maximum in the zone richest in the *PGE* and decrease outward (Fig. 7).

The second crystal (Table 4, Fig. 6b) shows certain differences (*cf.* Figs. 7 and 8), and Pd, not Rh, is the principal *PGE* in solid solution in this grain. The Co-rich zone (28.2 wt.% Co; 0.78 atoms per formula unit, *apfu*, Co) is located at the edge, the *PGE*-rich zone is in

TABLE 1. ELECTRON-MICROPROBE *(WDS)* DATA ON ZONED (PGE-RICH) COBALTITE-GERSDORFFITE-HOLLINGWORTHITE

	TRAVERSE A*							
No.	1	2	3	4	5	6	7	8**
	WEIGHT %							
Rh	1.69	6.90	13.10	6.67	5.82	2.23	1.34	3.97
Pd	1.35	2.70	4.16	2.55	2.62	1.93	1.30	2.35
Pt	0.35	0.71	1.77	0.94	0.97	0.68	0.54	0.44
Os	0.27	0.92	2.48	1.14	0.97	0.23	0.13	0.41
Ru	0.13	0.18	0.29	0.16	0.19	0.17	0.21	0.10
Co	16.65	10.80	8.28	9.84	9.79	13.93	18.21	10.29
Ni	9.52	11.46	8.00	12.26	12.83	11.52	8.57	13.93
Fe	5.90	5.71	4.27	5.42	5.53	5.68	5.41	5.99
As	44.51	43.52	41.95	43.07	43.59	44.43	44.43	44.44
S	19.00	18.09	16.80	18.19	18.08	18.34	19.12	17.92
Total	99.37	100.99	101.10	100.24	100.39	99.14	99.26	99.84
	ATOMIC PROPORTIONS (Σ atoms = 3)							
Rh	0.028	0.116	0.235	0.113	0.099	0.037	0.022	0.067
Pd	0.022	0.044	0.072	0.042	0.043	0.031	0.021	0.038
Pt	0.003	0.006	0.017	0.008	0.009	0.006	0.005	0.004
Os	0.002	0.008	0.024	0.010	0.009	0.002	0.001	0.004
Ru	0.002	0.003	0.005	0.003	0.003	0.003	0.004	0.002
Co	0.479	0.318	0.259	0.292	0.289	0.406	0.523	0.301
Ni	0.275	0.339	0.251	0.365	0.381	0.337	0.247	0.410
Fe	0.179	0.177	0.141	0.170	0.172	0.175	0.164	0.185
ΣM	0.990	1.011	1.004	1.003	1.005	0.997	0.987	1.011
As	1.007	1.008	1.031	1.005	1.013	1.019	1.004	1.024
S	1.004	0.979	0.965	0.992	0.982	0.983	1.010	0.965
As/S	1.00	1.03	1.07	1.01	1.03	1.04	0.99	1.06
100 Rh/(Rh + Pd)	56.0	72.5	76.5	72.9	69.7	54.4	51.2	63.8

* See Figure 6a for location of the electron-microprobe traverse A (# 1 to 7).
** Analysis # 8 refers to a zoned grain of cobaltite-gersdorffite (~ 15 μm). JEOL-8600 electron microprobe. Ir was sought, but not detected (<0.07 wt.% Ir).

TABLE 2. ELECTRON-MICROPROBE *(EDS)* DATA ON ZONED (PGE-RICH) COBALTITE-GERSDORFFITE-HOLLINGWORTHITE (TRAVERSE B*)

No.	1	2	3	4	5	6	7
	WEIGHT %						
Rh	2.62	4.58	16.88	5.24	3.21	1.05	0.86
Pd	1.76	2.54	4.65	2.33	2.14	1.52	0.97
Pt	n.a.	n.a.	1.86	n.a.	n.a.	n.a.	n.a.
Os	n.a.	n.a.	2.87	n.a.	n.a.	n.a.	n.a.
Co	14.09	11.43	6.22	10.60	11.67	17.82	22.69
Ni	10.91	12.08	6.20	12.63	12.79	9.31	5.77
Fe	5.69	5.60	3.48	5.32	5.55	5.36	4.11
As	46.73	46.73	41.75	46.70	46.95	47.34	47.08
S	18.54	18.14	15.50	18.00	18.14	19.03	19.21
Total	100.34	101.10	99.41	100.82	100.45	101.43	100.69
	ATOMIC PROPORTIONS (Σ atoms = 3)						
Rh	0.043	0.076	0.318	0.087	0.053	0.017	0.014
Pd	0.028	0.041	0.085	0.038	0.034	0.024	0.015
Pt	-	-	0.018	-	-	-	-
Os	-	-	0.029	-	-	-	-
Co	0.405	0.331	0.205	0.309	0.338	0.502	0.641
Ni	0.315	0.351	0.205	0.369	0.372	0.263	0.164
Fe	0.173	0.171	0.121	0.164	0.170	0.159	0.123
ΣM	0.964	0.970	0.981	0.967	0.967	0.965	0.957
As	1.057	1.064	1.081	1.070	1.069	1.049	1.046
S	0.980	0.965	0.938	0.963	0.965	0.985	0.997
As/S	1.08	1.10	1.15	1.11	1.11	1.06	1.05
100 Rh/(Rh+Pd)	60.6	65.0	78.9	69.6	60.9	41.5	48.3

* See Figure 6a for location of the electron-microprobe traverse B (# 1 to 7). Quantitative energy-dispersion analyses; n.a.: not analyzed or not detected.

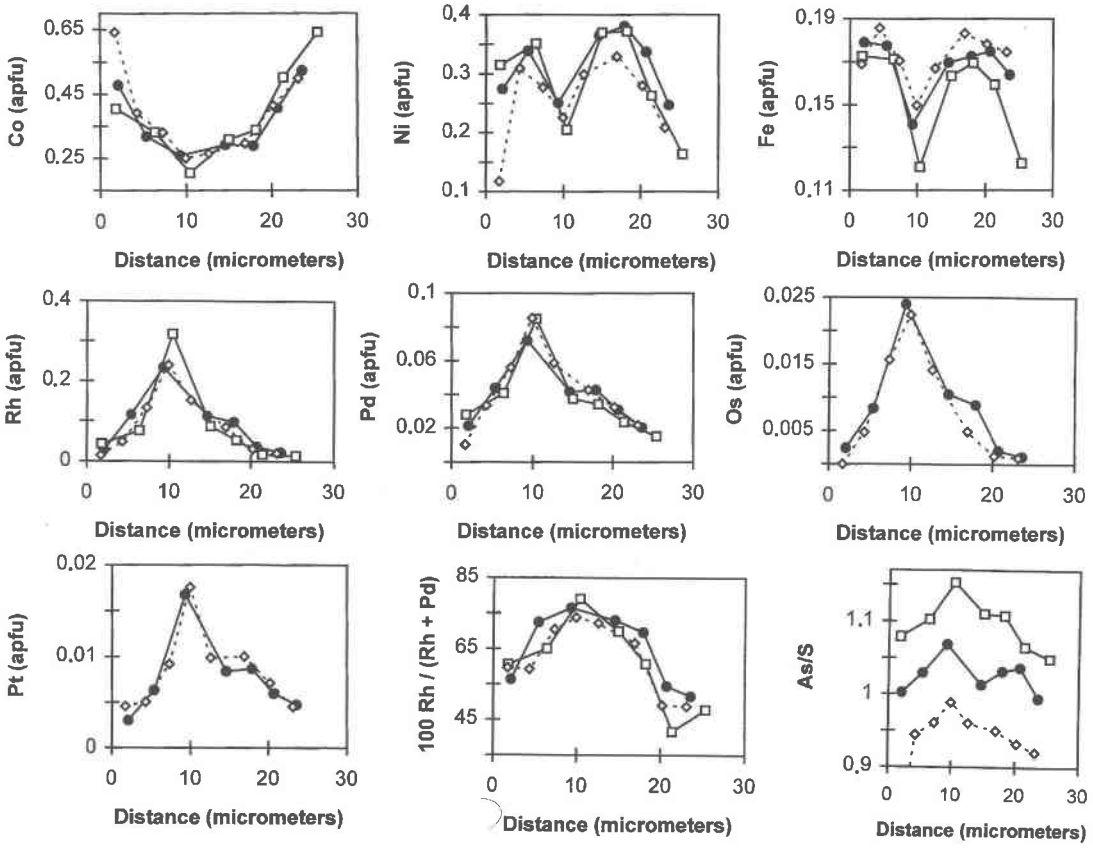

FIG. 7. Concentrations of elements (Co, Ni, Fe, Rh, Pd, Os, and Pt), in terms of atoms per formula unit, *apfu* (Σ atoms = 3), and variation in atomic ratios (X_{Rh} and As/S) along electron-microprobe traverses (A, B, and C) across the zoned grain shown in Figure 2a. See Figure 6a for location of these traverses and for the key to the symbols.

the center of the grain, and there is a general covariation of Ni, Fe and As/S, all of which vary antipathetically with Co. The zone richest in Co (24.6 wt.% Co; 0.70 *apfu* Co) in the third crystal also is at the edge, and the *PGE* gradually decrease toward the Co-rich edge (Fig. 6c, #4 to 7, Table 5). A noteworthy feature is the unusually Os-rich composition (11.3 wt.% Os) of the subhedral hollingworthite that is enclosed within this *MCGS*.

Type-II zoning

The central sulfarsenide (Hol-1, Figs. 2d, e) in the type-II zoned grain is rich in Ir and Pt (hollingworthite–irarsite). The second crystal (Hol-2) consists of an Ir-free (<0.07 wt.% Ir) hollingworthite. The outermost phase is a *PGE*-poor *MCGS* (Table 6). Both the hollingworthite–(irarsite) phases are poor in Co and Ni. Thus, the heavy *PGE* (Ir and Pt) are relatively enriched in the central sulfarsenide, the light *PGE* (Rh and Pd) in the surrounding sulfarsenide, and the transition metals in the outermost sulfarsenide. Typically, relative enrichment in the heavy *PGE* occurs in minute zones in the center (*e.g.*, Figs. 3a, b, f).

Element correlations in the PGE-bearing cobaltite–gersdorffite

This part of our study aimed to elucidate element-correlation relationships in the zoned *MCGS* containing low to moderate levels of the *PGE*. Thus, compositions close to end-member *PGE* sulfarsenides were omitted, and the composition richest in the *PGE*, which was used to calculate the correlation coefficient (R), is that given in Table 1, #3. To avoid additional analytical errors, results of 22 WDS analyses of the crystals (~20 μm), all of which were carried out with the JEOL–8600 electron microprobe, were selected on this basis (Table 1,

TABLE 3. ELECTRON-MICROPROBE *(WDS)* DATA ON ZONED (PGE-RICH) COBALTITE-GERSDORFFITE-HOLLINGWORTHITE **(TRAVERSE C*)**

No.	1	2	3	4	5	6	7	8
				WEIGHT %				
Rh	0.93	2.97	7.80	13.36	8.88	5.12	1.93	1.29
Pd	0.65	2.11	3.38	4.90	3.53	2.65	2.07	1.40
Pt	0.55	0.58	1.02	1.85	1.09	1.14	0.83	0.53
Os	n.d.	0.54	1.69	2.30	1.52	0.53	0.14	0.11
Co	23.42	13.67	11.02	7.97	8.82	10.17	14.58	17.76
Ni	4.26	10.76	9.24	7.16	9.92	11.25	9.82	7.38
Fe	5.84	6.14	5.40	4.52	5.27	5.96	5.94	5.88
As	41.57	43.50	41.81	40.43	42.17	43.55	44.32	44.79
S	22.78	19.73	18.64	17.51	18.81	19.64	20.37	20.85
				ATOMIC PROPORTIONS (Σ atoms = 3)				
Rh	0.015	0.049	0.134	0.240	0.153	0.085	0.031	0.021
Pd	0.010	0.033	0.056	0.085	0.059	0.043	0.033	0.022
Pt	0.005	0.005	0.009	0.018	0.010	0.010	0.007	0.004
Os	-	0.005	0.016	0.022	0.014	0.005	0.001	0.001
Co	0.642	0.392	0.330	0.250	0.265	0.296	0.414	0.500
Ni	0.117	0.310	0.277	0.226	0.299	0.329	0.280	0.208
Fe	0.169	0.186	0.170	0.150	0.167	0.183	0.178	0.175
ΣM	0.958	0.980	0.992	0.991	0.967	0.951	0.944	0.931
As	0.896	0.981	0.984	0.999	0.996	0.998	0.991	0.991
S	1.147	1.040	1.024	1.011	1.038	1.051	1.064	1.078
As/S	0.78	0.94	0.96	0.99	0.96	0.95	0.93	0.92
100 Rh / (Rh+Pd)	60.0	59.8	70.5	73.8	72.2	66.4	48.4	48.8

* Cameca Camebax electron microprobe. Analyses # 1 to 8 (normalized to 100 wt.%) refer to zoned grain in Figure 6a (path of this profile is close to those shown in Fig. 6a). Ir was sought, but not detected; n.d.: not detected.

TABLE 4. ELECTRON-MICROPROBE *(WDS)* DATA ON ZONED (PGE-BEARING) COBALTITE-GERSDORFFITE **(TRAVERSE D*)**

No.	1	2	3	4	5	6
			WEIGHT %			
Rh	n.d.	n.d.	0.42	0.09	n.d.	n.d
Pd	0.34	0.59	2.20	2.31	1.82	1.48
Pt	n.d.	n.d.	n.d.	n.d.	0.10	n.d.
Os	n.d.	n.d.	0.87	0.51	0.06	n.d.
Ru	n.d.	n.d.	0.15	0.16	0.12	n.d.
Co	28.23	26.18	19.89	19.38	19.25	19.32
Ni	4.94	6.04	8.85	9.53	10.21	9.96
Fe	2.94	3.42	4.85	5.11	5.40	5.71
As	44.78	44.95	44.39	44.44	44.77	44.66
S	19.66	19.54	19.35	19.25	19.22	19.25
Total	100.89	100.72	100.97	100.78	100.95	100.38
			ATOMIC PROPORTIONS (Σ atoms = 3)			
Rh	-	-	0.007	0.001	-	-
Pd	0.005	0.009	0.034	0.036	0.028	0.023
Pt	-	-	-	-	<0.001	-
Os	-	-	0.008	0.004	<0.001	-
Ru	-	-	0.002	0.003	0.002	-
Co	0.785	0.731	0.562	0.547	0.540	0.543
Ni	0.138	0.169	0.251	0.270	0.288	0.281
Fe	0.086	0.101	0.145	0.152	0.160	0.169
ΣM	1.014	1.010	1.009	1.013	1.019	1.016
As	0.980	0.987	0.986	0.987	0.989	0.988
S	1.005	1.003	1.005	0.999	0.992	0.995
As/S	0.975	0.98	0.98	0.99	1.00	0.99
100 Rh / (Rh + Pd)	0.0	0.0	17.1	2.7	0.0	0.0

* See Figure 6b for location of the electron-microprobe traverse D (# 1 to 6). JEOL-8600 electron microprobe. Ir was sought, but not detected (<0.07 wt.% Ir); n.d.: not detected.

#1 to 8; Table 4, #1 to 6; Table 5, #2 to 7, and Table 8, #1). The strongest correlations involve Co–Fe, Co–Ni, and Ni–Fe (Table 7, Fig. 9). Strong negative Co–As (and Co–As/S) and positive Co–S correlations, good positive correlations of all of the *PGE* (and Ni–Fe) with As and with As/S, and their negative correlations with S, should be particularly emphasized. In agreement, the EDS results (Table 2) show strong correlations involving Rh–As and Pd–As (R = 0.82 and 0.88), Rh–As/S and Pd–As/S (R = 0.87 and 0.93), Rh–S and Pd–S (R = –0.88 and –0.94), and Co–As and Co–S (R = –0.96 and 0.96). Strong positive correlations among the *PGE* (Table 7) indicate that they have behaved similarly during the crystallization.

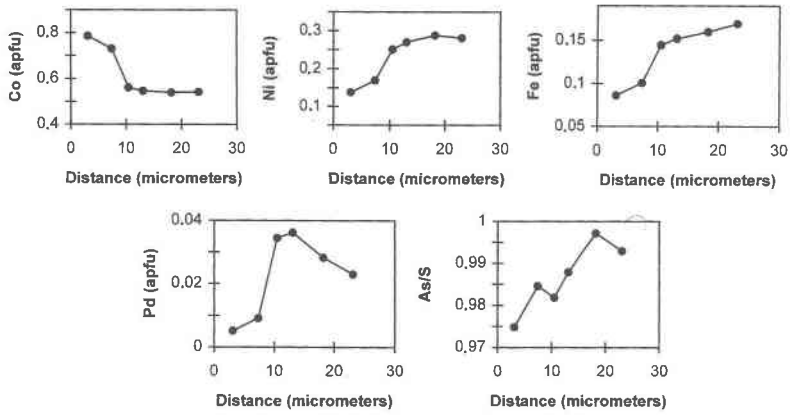

FIG. 8. Electron-microprobe traverse for Co, Ni, Fe, and Pd (*apfu*), and variation in the ratio As/S along this traverse, across the zoned grain shown in Figure 6b (traverse D).

TABLE 5. ELECTRON-MICROPROBE *(WDS)* DATA ON ZONED (PGE-RICH) COBALTITE-GERSDORFFITE-HOLLINGWORTHITE (TRAVERSE E*)

No.	1	2	3	4	4-A	5	6	7
				WEIGHT %				
Rh	18.80	0.87	2.56	2.54	1.86	1.03	0.11	n.d.
Pd	1.66	0.75	1.16	1.12	0.93	0.77	0.57	0.05
Pt	13.72	0.31	0.62	0.63	0.54	0.27	n.d.	0.16
Os	11.27	0.08	0.98	0.97	0.76	0.20	n.d.	n.d.
Ir	1.98	n.d.	0.15	0.15	n.d.	n.d.	n.d.	n.d.
Ru	1.29	0.08	0.14	0.13	0.10	0.10	0.05	n.d.
Co	1.68	11.89	10.13	10.08	10.77	12.17	11.89	24.56
Ni	2.11	15.77	16.02	15.96	16.05	15.57	16.92	6.00
Fe	1.66	6.06	5.68	5.66	5.64	5.89	5.84	4.53
As	32.09	45.83	45.27	44.78	43.91	44.23	44.77	44.42
S	14.02	18.82	18.79	18.69	18.54	18.91	18.72	19.16
Total	100.28	100.46	101.50	100.71	99.10	99.14	98.87	98.88
				ATOMIC PROPORTIONS (Σ atoms = 3)				
Rh	0.418	0.014	0.042	0.042	0.031	0.017	0.002	-
Pd	0.036	0.012	0.018	0.018	0.015	0.012	0.009	<0.001
Pt	0.161	0.003	0.005	0.005	0.005	0.002	-	0.001
Os	0.136	<0.001	0.009	0.009	0.007	0.002	-	-
Ir	0.024	-	0.001	0.001	-	-	-	-
Ru	0.029	0.001	0.002	0.002	0.002	0.002	<0.001	-
Co	0.065	0.337	0.289	0.290	0.312	0.348	0.340	0.698
Ni	0.082	0.449	0.459	0.461	0.467	0.448	0.485	0.171
Fe	0.068	0.181	0.171	0.172	0.173	0.178	0.176	0.136
ΣM	1.019	0.998	0.996	1.000	1.012	1.009	1.013	1.007
As	0.980	1.022	1.016	1.013	1.001	0.996	1.005	0.993
S	1.001	0.980	0.986	0.988	0.988	0.995	0.982	1.000
As/S	0.98	1.04	1.03	1.03	1.01	1.00	1.02	0.99
100 Rh / (Rh + Pd)	92.1	53.8	70.0	70.0	67.4	58.6	18.2	0.0

* See Figure 6c for location of the electron-microprobe traverse E (# 1 to 7). Analysis # 4-A was carried out adjacent to the analysis # 4. JEOL-8600 electron microprobe; n.d.: not detected.

TABLE 6. ELECTRON-MICROPROBE *(WDS)* DATA ON ZONED HOLLINGWORTHITE-COBALTITE-GERSDORFFITE

	WEIGHT %				ATOMIC PROPORTIONS (Σ atoms = 3)		
Zone*	Hol-1	Hol-2	Cob		Hol-1	Hol-2	Cob
Rh	18.77	36.31	0.24	Rh	0.431	0.721	0.004
Ir	22.59	n.d.	n.d.	Ir	0.277	-	-
Pd	0.41	0.97	0.22	Pd	0.009	0.019	0.003
Pt	7.84	4.73	0.28	Pt	0.095	0.049	0.002
Os	0.72	0.60	n.d.	Os	0.009	0.007	-
Ru	0.08	0.16	n.d.	Ru	0.002	0.003	-
Co	1.72	3.40	22.43	Co	0.069	0.118	0.628
Ni	1.00	1.21	9.18	Ni	0.040	0.042	0.258
Fe	1.09	1.28	3.87	Fe	0.046	0.047	0.114
As	32.26	36.03	43.68	ΣM	0.978	1.006	1.009
S	13.65	15.87	19.94	As	1.017	0.983	0.963
Total	100.13	100.56	99.84	S	1.005	1.011	1.027
			As/S		1.01	0.97	0.94
			100 (Ir + Pt) / (Ir + Pt + Rh)		46.3	6.4	-

* Zones shown in Figures 2d,e. Hol: hollingworthite, Cob: cobaltite-gersdorffite. JEOL-8600 electron microprobe; n.d.: not detected.

Minerals in complementary relations

Representative compositions of merenskyite and *MCGS*, which occur in complementary textural relationships (Figs. 5a,b), are given in Table 8. The *MCGS*, which is partially rimmed by merenskyite (Fig. 5a), contains elevated *PGE* in solid solution, whereas the partial rim of *MCGS* around merenskyite (Fig. 5b) is Co-rich. Both grains of merenskyite are similar in composition, except for a zone poorer in Bi in the grain shown in Figure 5b (Table 8, #7).

Comparison with Other Occurrences

The *MCGS* at General'skaya contain up to ~12 atom.% of Σ*PGE*, mainly Rh and Pd. In terms of their *PGE* content, the *MCGS* richest in *PGE* from this complex are comparable with those from Karik'yavr, Pipe and Lukkulaisvaara, where similar *MCGS*, containing more than 5 wt.% of the Σ*PGE*, have been previously recorded. At Karik'yavr (Kola Peninsula, Russia), the *MCGS* contain both Rh and heavy *PGE* (Distler & Laputina 1979). At Pipe in Manitoba and at Lukkulaisvaara (Russian Karelia), the *MCGS* contain up to 7 wt.% Rh (Cabri 1992) and 9 wt.% Rh (Barkov *et al.* 1996), respectively. The latter authors reported a transitional member in the hollingworthite – cobaltite – gersdorffite series and suggested a possibility of continuous solid-solution between the Co–Ni–(Fe) and *PGE* sulfarsenides. More recently, *PGE*-rich *MCGS* have been described from Argentina (Gervilla *et al.* 1997). It is noteworthy that most of the *PGE*-rich *MCGS* occurrences known to date (*i.e.*, Karik'yavr, Lukku-

TABLE 7. CORRELATION MATRIX FOR (PGE-BEARING) COBALTITE–GERSDORFFITE*

	Fe	Co	Ni	Rh	Pd	Pt	Os	Ru	ΣPGE	X_{Rh}	As	S	As/S
Fe	+++	–0.79	0.78	0.16	0.22	0.22	0.09	0.34	0.18	0.61	0.57	–0.46	0.55
Co		+++	–0.84	–0.60	–0.48	–0.65	–0.58	–0.59	–0.60	–0.86	–0.78	0.75	–0.81
Ni			+++	0.10	–0.01	0.18	0.14	0.16	0.09	0.60	0.52	–0.54	0.55
Rh				+++	0.83	0.94	0.90	0.75	0.99	—	0.64	–0.66	0.69
Pd					+++	0.73	0.80	0.82	0.89	—	0.46	–0.55	0.53
Pt						+++	0.86	0.80	0.93	0.76	0.70	–0.60	0.69
Os							+++	0.76	0.92	0.61	0.53	–0.53	0.56
Ru								+++	0.80	0.65	0.55	–0.39	0.50
ΣPGE									+++	0.66	0.62	–0.64	0.67
X_{Rh}										+++	0.80	–0.57	0.74
As											+++	–0.79	---

* WDS electron-microprobe data; $n = 22$ (JEOL-8600 microprobe). X_{Rh} = 100Rh/(Rh + Pd).

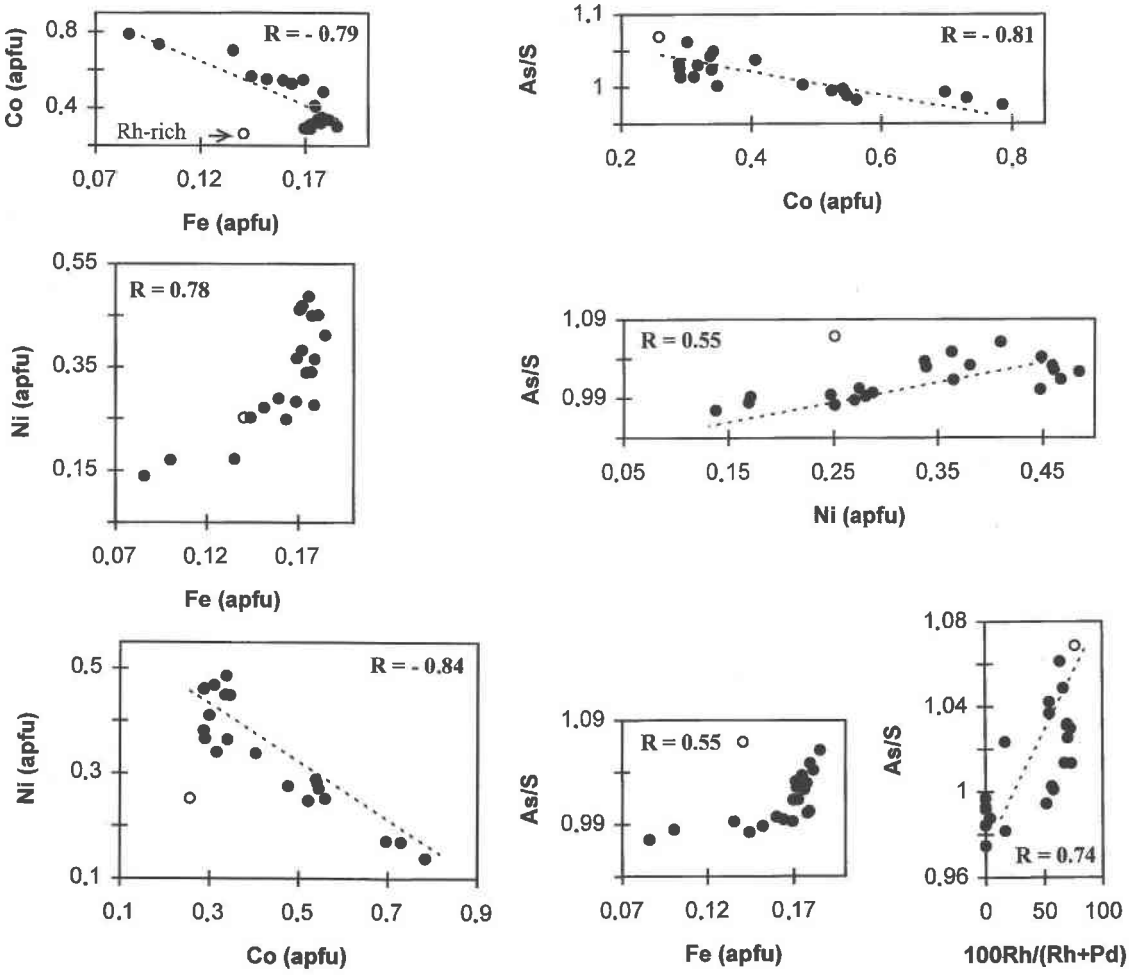

FIG. 9. Correlation diagrams (*apfu*) for *PGE*-bearing cobaltite–gersdorffite from Mount General'skaya; $n = 22$ (JEOL–8600 electron microprobe; solid circles). The composition richest in the *PGE* (diffuse core; Fig. 2a) is shown by an open symbol.

laisvaara and Mount General'skaya) are in the northeastern Fennoscandian Shield. A few other occurrences of the *MCGS* with ΣPGE less than 5 wt.% are known (Cabri 1992).

Zoned *PGE* sulfarsenides (type-II zoning) are not so rare. Genkin *et al.* (1966) and Rucklidge (1969) described zoned crystals with a core of irarsite and a rim of hollingworthite from Bushveld and Werner Lake (Ontario), respectively. Häkli *et al.* (1976) described a complexly zoned grain from Hitura (Finland); it consists of a Bi–Te phase and iridarsenite in the core, which are rimmed by successive zones of irarsite, Ir-free hollingworthite and a *MCGS*. Cabri (1981) noted the general heterogeneity of natural *PGE*-sulfarsenides ranging in composition from hollingworthite to irarsite, which is usually at the center. Cabri (1986) provided a micrograph of a zoned grain from Sudbury, consisting of subhedral irarsite, which is surrounded by hollingworthite, and the outermost *MCGS*. Volborth *et al.* (1986) documented Ir-rich zones in the central part of a minute grain of hollingworthite from Stillwater. Tarkian & Prichard (1987) noted the presence of a rim of hollingworthite around irarsite from the Shetland ophiolite complex, and proposed "an increase in availability Rh at the expense of Ir" in the environment. Halkoaho *et al.* (1990) described a core of irarsite rimmed by hollingworthite from Penikat (Finland).

TABLE 8. ELECTRON-MICROPROBE DATA ON COBALTITE-GERSDORFFITE AND MERENSKYITE IN COMPLEMENTARY TEXTURAL RELATIONSHIPS

No.	1	2*	3	4	5	6	7
	WDS *Cob*	EDS *Cob*	WDS *Mer*	EDS *Mer*	EDS *Cob*	EDS *Mer*	EDS *Mer*
				WEIGHT %			
Rh	3.61	2.50	n.d.	n.a.	n.d.	n.a.	n.a.
Pd	1.89	1.59	25.89	27.27	n.d.	25.26	24.43
Pt	0.44	n.a.	n.d.	n.d.	n.d.	n.d.	n.d.
Os	0.82	n.a.	n.a.	n.a.	n.d.	n.a.	n.a.
Ru	0.11	n.a.	n.a.	n.a.	n.d.	n.a.	n.a.
Co	11.63	13.44	n.a.	n.a.	24.30	n.a.	n.a.
Ni	12.31	11.33	0.33	n.d.	5.40	1.21	2.04
Fe	5.78	5.70	0.15	n.a.	4.02	n.a.	n.a.
Te	n.a.	n.a.	58.76	60.80	n.a.	58.95	68.71
Bi	n.a.	n.a.	13.06	12.83	n.a.	14.69	4.44
As	44.50	46.88	n.a.	n.a.	48.17	n.a.	n.a.
S	18.16	18.33	n.a.	n.a.	19.58	n.a.	n.a.
Total	99.25	99.77	98.19	100.90	101.47	100.11	99.62
				ATOMIC PROPORTIONS (Σ atoms = 3)			
Rh	0.061	0.04	-	-	-	-	-
Pd	0.031	0.03	0.94	0.97	-	0.90	0.84
Pt	0.004	-	-	-	-	-	-
Os	0.007	-	-	-	-	-	-
Ru	0.002	-	-	-	-	-	-
Co	0.342	0.39	-	-	0.68	-	-
Ni	0.363	0.33	0.02	-	0.15	0.08	0.13
Fe	0.179	0.17	0.01	-	0.12	-	-
ΣM	0.989	0.96	0.97	0.97	0.95	0.98	0.97
Te	-	-	1.78	1.80	-	1.75	1.96
Bi	-	-	0.24	0.23	-	0.27	0.08
Te + Bi	-	-	2.02	2.03	-	2.02	2.04
As	1.029	1.07	-	-	1.05	-	-
S	0.981	0.97	-	-	1.00	-	-

Analyses *#1* to *4* (see Fig. 5a), *#5* to *7* (Fig. 5b). *#1, 2:* cobaltite-gersdorffite (Cob), *#3, 4:* partial rim of merenskyite (Mer) around this cobaltite-gersdorffite. Partial rim of cobaltite-gersdorffite (Cob; *#5*) around merenskyite (Mer; *#6*); *#7:* Bi-poor zone in the latter merenskyite. WDS: WDS electron-microprobe analyses; EDS: EDS electron-microprobe analyses; n.d.: not detected; n.a.: not analyzed.
* Analysis carried out far enough from *PGE*-rich zone (Fig. 5a).

Discussion and Conclusions

Substitutions in PGE-bearing cobaltite–gersdorffite

The type-I zoning in the General'skaya *MCGS* is unlike that of other natural Co–Ni–*PGE* sulfarsenides described in the literature. Compositional variations along the electron-microprobe traverses and the element correlations reveal the following characteristics: (1) all of the *PGE* substitute isomorphously for Co, not for Ni and Fe; (2) the *PGE* correlate positively with As (and As/S), and they are selectively incorporated in relatively As-rich (S-poor) *MCGS*; (3) an increase in Rh relative to Pd is accompanied by an increase in As relative to S; (4) Fe substitutes for Co, not Ni, and also shows a preference for zones richer in As; (5) similarly, Ni is relatively enriched in zones richer in As (S-poor); (6) in contrast to all the other metals, only Co shows a strong positive correlation with S and is preferentially incorporated in relatively S-rich (As-poor) *MCGS*, and (7) the common Co–Ni substitution is indicated by inverse correlation between these elements in the zoned *MCGS*. Figure 10 shows their compositions plotted in the CoAsS – FeAsS – NiAsS system. The crystallization trend extends along the Ni/Fe = 2 line, and the average Ni:Fe atomic ratio is 2.0 (n = 21), suggesting that the zoned *MCGS* form a solid solution between CoAsS and $(Ni_{0.667}Fe_{0.333})AsS$, and an ordered distribution of Ni and Fe probably exists in their crystal structure (*cf.* Béziat *et al.* 1996).

Though the variations in As:S ratio are quite limited, As and S display the strong negative correlation (R = –0.8) indicative of their mutual substitution. Related variations in the metals and As:S ratio (Fig. 7) indicate a link between cation and anion substitutions in the *MCGS*. The possible presence of As and S in *MCGS* in the form of $[AsS]^{3-}$ paired dianion is suggested by the data of Wood & Strens (1979). These authors concluded that in related pyrite-type compounds, in various disulfides, sulfarsenides and diarsenides of transition metals, the existing dianions are $[S_2]^{2-}$, $[AsS]^{3-}$ and $[As_2]^{4-}$, respectively, and they require corresponding formal positive charges (2, 3 and 4, respectively) on the metals in order to maintain charge balance. An increase in the cobaltite end-member in the General'skaya *MCGS* leads to a decrease in the As:S ratio, and the compositions richest in Co are relatively S-rich (Fig. 9). The predominance of S over As should be stronger in *MCGS* closer to the CoAsS-rich end-member in this series. In contrast, an increase in gersdorffite (and Fe) leads to an increase in the As:S ratio, both in *PGE*-enriched (Fig. 9) and *PGE*-poor *MCGS* (Fig. 8), which contain minor Pd. These findings are corroborated by compositions of (*PGE*-free) *MCGS* from Lacaune, France (see Table 1 in Béziat *et al.* 1996), as the latter display strong positive Ni–As/S and Fe–As/S correlations (R = 0.9 and 0.8), along with an inverse Co–As/S correlation (R = –0.9; this study).

Large variations in As:S ratio are known in both synthetic and natural gersdorffite- and cobaltite-rich sulfarsenides. In the system Ni–As–S, the gersdorffite solid-solution extends along a line from rammelsbergite (or pararammelsbergite), $NiAs_2$, to vaesite (NiS_2); however, most of this solid solution extends toward $NiAs_2$, and natural examples form an extensive series toward rammelsbergite (Yund 1962). Synthetic cobaltite (Bayliss 1969) displays a continuous solid-solution from CoAsS (a = 5.58 Å) to $Co_{1.0}S_{1.6}As_{0.4}$ (a = 5.56 Å). Apparently, the latter phase is related to cattierite, CoS_2 (pyrite group; a = 5.54 Å; PDF 41–1471). Maurel & Picot (1974) also noted that cobaltite readily accommodates an excess in S over As, but no excess in As over S. Thirteen samples belonging to the gersdorffite series (≤0.02 *apfu* Sb) and 13 samples of cobaltite (Bayliss 1982a, b) show wide ranges in the ratio As:S, from 0.97 to 2.46, mean 1.32, and from 1.03 to 0.78, mean 0.93, respectively (this study). The gersdorffite richest in As has the composition $(Ni_{0.82}Fe_{0.11}Co_{0.07})_{\Sigma 1.00}(As_{1.42}S_{0.58}Sb_{0.01})_{\Sigma 2.01}$. As these samples are from different localities worldwide (Bayliss 1982a, b), they are likely quite representative, and suggest that natural gersdorffite and cobaltite commonly form different

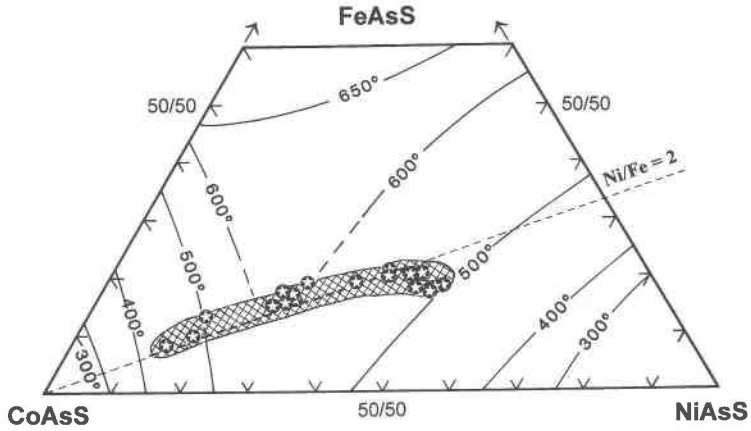

FIG. 10. Crystallization trend of zoned cobaltite–gersdorffite from the Mount General'skaya complex (JEOL–8600 electron microprobe). Both *PGE*-poor and *PGE*-rich compositions (≤7 wt.% Rh, ≤3 wt.% Pd, and ≤1 wt.% Pt or Os) are plotted, with reference to the solvus in the system CoAsS – FeAsS – NiAsS, mol.% (Klemm 1965). $n = 21$; two points are hidden.

solid-solution series, extending toward $NiAs_2$ and toward CoS_2, respectively.

On the basis of the findings of Wood & Strens (1979), it is reasonable to suppose that some of the anion pairs in As-excess gersdorffite–(rammelsbergite) are $[As_2]^{4-}$ pairs, which substitute for $[AsS]^{3-}$ pairs, and this substitution is coupled with a Me^{4+}-for-Me^{3+} substitution to maintain charge balance. The cobaltite–(cattierite) series implies another scheme of substitution, $Co^{2+} + [S_2]^{2-} = Co^{3+} + [AsS]^{3-}$. If so, in order to maintain electroneutrality, totals of the formal positive charges on participating metals and corresponding As/S values of gersdorffite–(rammelsbergite)-rich *MCGS* should be higher than those of cobaltite–(cattierite)-rich *MCGS*. The relative increase in the As/S value in Ni-rich (Co-poor) *MCGS* at General'skaya is consistent with this suggestion, and implies that members in this series richest in cobaltite and in (*PGE*-rich)-gersdorffite may have cattierite $[Co]^{2+}[S_2]^{2-}$ and diarsenide $[Me]^{4+}[As_2]^{4-}$ components, respectively. Nickel may be primarily responsible for the positive Fe–As/S correlation, as Ni–Fe order appears to exist in these *MCGS*, and Fe is linked with Ni and increases as Ni increases. Charge-balanced substitutions also appear to control incorporation of the *PGE* in the As-rich *MCGS*. When the *PGE* (Rh, tetravalent heavy *PGE* and Ru) enter the cobaltite-type structure, a charge imbalance appears, which probably is compensated by the increase in As relative to S (Table 7, Figs. 7, 9) by means of limited substitution of $[As_2]^{4-}$ for $[AsS]^{3-}$. Related mechanisms involving anions (As^{3-} and S^{2-}) in charge compensation are alternatives to the dianion substitutions, but these are less probable.

Substitutions involving dianions also may be operative in other *PGE*-rich sulfarsenides, *e.g.*, in Rh–(S)-bearing sperrylite–(hollingworthite) from Nomgon, Mongolia, which contains from less than 0.1 to ~0.4 *apfu* Rh and S, and displays nearly linear positive Rh–S correlation with the ratio Rh:S of ~1 (Izokh & Mayorova 1990). We suggest that these variations may be governed by the charge-balanced mechanism $Rh^{3+} + [AsS]^{3-} \rightarrow Pt^{4+} + [As_2]^{4-}$.

Owing to the small grain-size, no XRD data could be obtained for the General'skaya *PGE*-bearing *MCGS*, and their symmetry remains unknown. Cobaltite and hollingworthite – irarsite – platarsite are not isostructural, though closely related. Cobaltite only crystallizes with the orthorhombic (pseudocubic) $Pca2_1$ structure (Bayliss 1982b), the *PGE* sulfarsenides crystallize with the cubic symmetry of the *Pa*3 structure, and gersdorffite crystallizes with various structures (*Pa*3, $Pca2_1$, and $P2_13$), whose fields of stability probably are temperature-dependent (Bayliss 1982a).

Origin of the zoning

The zoning patterns in the Co–Ni–(Fe)–*PGE* sulfarsenides from General'skaya indicate that (1) all the *PGE* present are selectively enriched in the earlier (typically in central) sulfarsenide phase, relative to the periphery, and their content gradually (type-I zoning) or sharply (type-II zoning) decreases toward the edge, and (2) the type-II zoning demonstrates that the heavy *PGE* (Ir and Pt) are more effectively partitioned into the earliest phase (typically in the core) than Rh. The examples cited from the literature strongly suggest that this

is a general feature, which also is corroborated by a cryptic zoning in a rim (~ 40 μm) of Rh-rich irarsite around laurite from the Penikat complex (Barkov & Halkoaho, unpubl. data). The rim shows a decrease in the irarsite component (and an increase in the hollingworthite component) toward the edge; in terms of the irarsite (Irs), hollingworthite (Hol) and ruarsite (Rs) end-members, the compositional ranges are $Irs_{69.9}Hol_{22.4}Rs_{7.7}$ → $Irs_{69.3}Hol_{25.0}Rs_{5.7}$ → $Irs_{65.5}Hol_{28.8}Rs_{5.7}$ → $Irs_{55.3}Hol_{40.5}Rs_{4.2}$. Monoclinic sulfarsenides, ruarsite RuAsS and OsAsS, may partly substitute for hollingworthite (Barkov *et al.* 1996).

The General'skaya patterns also demonstrate that transition metals (Co, Ni, and Fe) are strongly concentrated in the latest, marginal phases. The extreme variations in Co are of particular interest. The entire range of Co content in the zoned grains at General'skaya (*e.g.*, 6–23 wt.% Co) is comparable to that obtained for a large number of the *MCGS* grains from Sudbury (3–21 wt.% Co; Cabri & Laflamme 1976). The type-I zoning at General'skaya reveals that X_{Rh} systematically decreases toward the edge. This index may thus reflect a more evolved (probably lower-*T*) character of the *MCGS*, with a low X_{Rh}. Similar ratios involving the other *PGE* present [*e.g.*, X_{Ir} = 100 Ir(+Pt) / Ir (+ Pt) + Rh], as implied in the type-II zoning, or ΣPGE / Σ(*PGE*, Ni, Co, Fe)], may also be useful for related sulfarsenides.

The textural and compositional evidence, along with the general similarity in type-II zoning at General'skaya and in other complexes, strongly argue for a primary origin of the zoning and for the same major factor(s) responsible for the zoning. The term *primary* is used here to note that the zoned grains at General'skaya were not formed by alteration reactions, but rather crystallized from single micro-volumes of late-stage liquids or fluids, under closed-system conditions, unlike the *PGE* sulfarsenides from Two Duck Lake, in the Coldwell Complex, Ontario, whose zoning reflects "effects of fluids that may have transported and precipitated different proportions of the *PGE* at different times" (Ohnenstetter *et al.* 1991). The primary character of the zoning at General'skaya is evident from (1) the internal arrangement of the zoned grains and their well-developed growth-related zoning, which is parallel or subparallel to crystal faces (Figs. 2, 3), (2) the lack of alteration of early-formed zones, in contrast to the Two Duck Lake sulfarsenides, which display strongly irregular zoning and "late dissolution and replacement along cracks and at the edges of the grains" (Ohnenstetter *et al.* 1991), (3) the cryptic zoning and continuous compositional trends, which indicate gradual (evolutionary) changes with progressive crystallization (*e.g.*, Fig. 7), and (4) the crystallization trend of the General'skaya *MCGS* in the system CoAsS – FeAsS – NiAsS after Klemm (1965) (Fig. 10), which suggests the lowest *T* (≤450–500°C) for the *MCGS* composition richest in the cobaltite end-member and poorest in *PGE* at the edges. These findings are in accord with the textural data and imply that the *PGE*-rich zones crystallized first, and most of the zoned grains crystallized from the center to the edge, or from the *PGE*-rich to the *PGE*-poor zones.

The type-I zoning and the remarkable similarity in the type-II zoning at General'skaya and other localities strongly imply that the temperature of formation (*i.e.*, differences in the *T* of crystallization of the end-member *PGE*–Co–Ni sulfarsenides) could exert a major control over the zoning, whereas variations in activities of the mineral-forming elements (*X*) could be of lesser importance. Formation of the zoned patterns may thus be explained in terms of decreasing *T* and changing *X* during crystallization (rather gradually for type-I and sharply for type-II zoning). Unfortunately, detailed experimental work on the Co–Ni–(Fe)–*PGE* sulfarsenide systems is lacking, and no exact experimentally determined stability-limits of the *PGE* sulfarsenides are so far known. The uniformly zoned sulfarsenides at General'skaya and in other localities suggest a higher *T* of crystallization for the Ir–(Pt) sulfarsenides, a lower *T* for the Rh–(Pd) sulfarsenides, and the lowest *T* for the Co–Ni–(Fe) sulfarsenides. A relatively high-*T* character of RhAsS *versus* (Rh,Pd)AsS also may be implied by the decrease in the X_{Rh} values during crystallization.

Implications from complementary relationships

Compositions and complementary replacement relationships between the *MCGS* and merenskyite may be useful to constrain their temperature of formation. The composition of the *MCGS* grain (partly surrounded by merenskyite; Fig. 5a, Table 8), plotted in the system CoAsS – FeAsS – NiAsS (Klemm 1965), yields a *T* close to 550°C. However, the actual *T* could be somewhat higher, because the *PGE* are present in solid solution. The partial rim of *MCGS* around merenskyite (Fig. 5b, Table 8), which is enriched in cobaltite, must have crystallized at a *T* of ~500°C, according to the experimental data of Klemm. The relatively low-*T* character of this *MCGS* is in good accord with its occurrence as the rim. Compositional similarities (Table 8) between the partial rim of Bi-rich merenskyite (around the *MCGS*) and the single grain of merenskyite (partly rimmed by the *MCGS*; Fig. 5) suggest that they crystallized at a rather similar temperature. According to experimental data (Hoffman & MacLean 1976), the melting point of merenskyite decreases with substitution of Bi for Te, from 740°C (stoichiometric $PdTe_2$) to 500–525°C ($Pd_{1.05}Te_{1.34}Bi_{0.61}$). Thus, the General'skaya compositions ($Pd_{0.90-0.97}Ni_{0.02-0.08}$)($Te_{1.75-1.80}Bi_{0.23-0.27}$) imply a *T* between 600 and 650°C. This estimate is in good agreement with that of *ca.* 500°C for the *MCGS* rim around the merenskyite, and suggests a *T* in excess of 600°C for the *PGE*-bearing *MCGS* (Fig. 5a), rimmed by the merenskyite. In summary, the General'skaya *MCGS* and associated merenskyite appear to have formed at a postmagmatic hydrothermal stage, nearly simultaneously, resulting in their mutual replacement relationship.

Source of the As

The relative abundance of *MCGS* (and other As-bearing minerals) in various complexes of the Pechenga structural unit, *i.e.*, Karik'yavr (Distler & Laputina 1979), Mount General'skaya (this study), and Pechenga gabbro–wehrlite intrusions (*e.g.*, Abzalov *et al.* 1997) may reflect an initial (relative) enrichment in As in their parental magmas, giving rise to As minerals in associated ores, in particular those formed at the latest stage, because of the strongly incompatible behavior of As. Alternatively, As could be introduced during *in situ* contamination by the wallrocks, as was suggested for the Pechenga ores, the main source of As being the host sulfide-bearing shales (Abzalov *et al.* 1997). The latter possibility seems, however, less likely in the case of the Mount General'skaya complex.

Acknowledgements

This study was supported by NSERC (Canada) and the Academy of Finland. We thank B. Cornelisen and M. Tarkian for some electron-microprobe analyses, and L.J. Cabri for providing PGE standards (EDS analysis). Reviews from F. Merchel, H.M. Prichard, and Associate Editor G. Garuti are appreciated. Particular thanks are due to R. F. Martin for his constructive comments, improvements and encouragement.

References

Abzalov, M.Z., Brewer, T.S. & Polezhaeva, L.I. (1997): Chemistry and distribution of accessory Ni, Co, Fe arsenic minerals in the Pechenga Ni–Cu deposits, Kola Peninsula, Russia. *Mineral. Petrol.* **61**, 145-161.

Amelin, Y.V., Heaman, L.M. & Semenov, V.S. (1995): U–Pb geochronology of layered mafic intrusions in the eastern Baltic Shield: implications for the timing and duration of Paleoproterozoic continental rifting. *Precambrian Res.* **75**, 31-46.

Bakushkin, Y.M. (1979): A copper-nickel sulfide deposit in the Mount General'skaya (Luostari) intrusion. *In* New Data on the Mineralogy of Copper–Nickel Ores in the Kola Peninsula. Kola Science Center, Geological Institute, Apatity, Russia (79-84; in Russ.).

_____, Zhuravlev, D.Z., Bayanova, T.B. & Balashov, Y.A. (1990): The Mount General'skaya. *In* Geochronology and Genesis of Layered Basic Intrusions, Volcanites and Granite-Gneisses of the Kola Peninsula. Kola Science Center, Geological Institute, Apatity, Russia (14-15; in Russ.).

Barkov, A.Y., Alapieti, T., Laajoki, K. & Peura, R. (1996): Osmian hollingworthite and rhodian cobaltite–gersdorffite from the Lukkulaisvaara layered intrusion, Russian Karelia. *Mineral. Mag.* **60**, 973-978.

_____, Bakushkin, Y.M. & Lednev, A.I. (1990): Platinum-group minerals from the Mount General'skaya intrusion. *In* All-Union Mineral. Soc. Conf. (Apatity), 33-34 (abstr., in Russ.).

_____, Lednev, A.I. & Bakushkin, Y.M. (1994): Platinum-group minerals from the Mount General'skaya layered intrusion, Kola Peninsula. *Dokl. Akad. Nauk* **338**, 785-788 (in Russ.).

Bayliss, P. (1969): Isomorphous substitution in synthetic cobaltite and ullmannite. *Am. Mineral.* **54**, 426-430.

_____ (1982a): A further crystal structure refinement of gersdorffite. *Am. Mineral.* **67**, 1058-1064.

_____ (1982b): A further crystal structure refinement of cobaltite. *Am. Mineral.* **67**, 1048-1057.

Béziat, D., Monchoux, P. & Tollon, F. (1996): Cobaltite – gersdorffite solid solution as a primary magmatic phase in spessartite, Lacaune area, Montagne Noire, France. *Can. Mineral.* **34**, 503-512.

Cabri, L.J. (1981): The platinum-group minerals. *In* Platinum-Group Elements: Mineralogy, Geology, Recovery (L.J. Cabri, ed.). *Can. Inst. Mining Metall., Spec. Vol.* **23**, 83-150.

_____ (1986): A third issue devoted to platinum deposits; Preface. *Econ. Geol.* **81**, 1045-1048.

_____ (1992): The distribution of trace precious metals in minerals and mineral products. *Mineral. Mag.* **56**, 289-308.

_____ & Laflamme, J.H.G. (1976): The mineralogy of the platinum-group elements from some copper – nickel deposits of the Sudbury area, Ontario. *Econ. Geol.* **71**, 1159-1195.

_____, _____ & Stewart, J.M. (1977): Platinum-group minerals from Onverwacht. II. Platarsite, a new sulfarsenide of platinum. *Can. Mineral.* **15**, 385-388.

Distler, V.V. & Laputina, I.P. (1979): Sulfarsenides of nickel and cobalt containing platinoids. *Dokl. Akad. Nauk SSSR* **248**, 718-721 (in Russ.).

Genkin, A.D., Zhuravlev, N.N., Troneva, N.V. & Murav'eva, I.V. (1966): Irarsite, a new sulfarsenide of iridium, rhodium, ruthenium and platinum. *Zap. Vses. Mineral. Obshchest.* **95**, 700-712 (in Russ.).

Gervilla, F., Sánchez-Anguita, A., Acevedo, R.D., Fenoll Hach-Alí, P. & Paniagua, A. (1997): Platinum-group element sulpharsenides and Pd bismuthotellurides in the metamorphosed Ni–Cu deposit at Las Aguilas (Province of San Luis, Argentina). *Mineral. Mag.* **61**, 861-877.

Häkli, T.A., Hänninen, E., Vuorelainen, Y. & Papunen, H. (1976): Platinum-group minerals in the Hitura nickel deposit, Finland. *Econ. Geol.* **71**, 1206-1213.

HALKOAHO, T.A.A., ALAPIETI, T.T. & LAHTINEN, J.J. (1990): The Sompujärvi PGE Reef in the Penikat layered intrusion, northern Finland. *Mineral. Petrol.* **42**, 39-55.

HOFFMAN, E. & MACLEAN, W.H. (1976): Phase relations of michenerite and merenskyite in the Pd–Bi–Te system. *Econ. Geol.* **71**, 1461-1468.

IZOKH, A.E. & MAYOROVA, O.N. (1990): A rhodium-bearing sperrylite from the Nomgon complex (Mongolia). *Dokl. Akad. Nauk SSSR* **313**, 1212-1215 (in Russ.).

KLEMM, D.D. (1965): Synthesen und Analysen in den Dreiecks-diagrammen FeAsS–CoAsS–NiAsS und FeS_2–CoS_2–NiS_2. *Neues Jahrb. Mineral., Abh.* **103**, 205-255.

MAUREL, C. & PICOT, P. (1974): Stabilité de l'alloclasite et de la cobaltite dans les systèmes Co–As–S et Co–Ni–As–S. *Bull. Soc. fr. Minéral. Cristallogr.* **97**, 251-256.

OHNENSTETTER, D., WATKINSON, D.H. & DAHL, R. (1991): Zoned hollingworthite from the Two Duck Lake intrusion, Coldwell complex, Ontario. *Am. Mineral.* **76**, 1694-1700.

RUCKLIDGE, J. (1969): Electron microprobe investigations of platinum-metal minerals from Ontario. *Can. Mineral.* **9**, 617-628.

STUMPFL, E.F. & CLARK, A.M. (1965): Hollingworthite, a new rhodium mineral, identified by electron probe microanalysis. *Am. Mineral.* **50**, 1068-1074.

TARKIAN, M. & PRICHARD, H.M. (1987): Irarsite – hollingworthite solid-solution series and other associated Ru-, Os-, Ir- and Rh-bearing PGM's from the Shetland ophiolite complex. *Mineral. Deposita* **22**, 178-184.

VOLBORTH, A., TARKIAN, M., STUMPFL, E.F. & HOUSLEY, R.M. (1986): A survey of the Pd–Pt mineralization along the 35-km strike of the J–M reef, Stillwater complex, Montana, USA. *Can. Mineral.* **24**, 329-346.

WOOD, B.J. & STRENS, R.G. (1979): Diffuse reflectance spectra and optical properties of some sulphides and related minerals. *Mineral. Mag.* **43**, 509-518.

YAKOVLEV, I.A. (1971): A new type of the copper – nickel sulfide deposit in basic rocks of the Luostari massif. *Razvedka i Okhrana Nedr.* **11**, 1-4 (in Russ.).

YUND, R.A. (1962): The system Ni–As–S: phase relations and mineralogical significance. *Am. J. Sci.* **260**, 761-782.

Received January 8, 1998, revised manuscript accepted October 15, 1998.